Environmental Science & Technology

Article

pubs.acs.org/est

Organic Carbon and Reducing Conditions Lead to Cadmium Immobilization by Secondary Fe Mineral Formation in a pH-Neutral Soil

E. Marie Muehe,[†] Irini J. Adaktylou,[†] Martin Obst,[‡] Fabian Zeitvogel,[‡] Sebastian Behrens,[†] Britta Planer-Friedrich,[§] Ute Kraemer,[∥] and Andreas Kappler*[,†]

[†]Geomicrobiology and [‡]Environmental Analytical Microscopy, Center for Applied Geosciences, University of Tuebingen, 72076 Tuebingen, Germany

[§]Environmental Geochemistry, University of Bayreuth, 95440 Bayreuth, Germany

[∥]Department for Plant Physiology, Ruhr University Bochum, 44801 Bochum, Germany

Supporting Information

ABSTRACT: Cadmium (Cd) is of environmental relevance as it enters soils via Cd-containing phosphate fertilizers and endangers human health when taken up by crops. Cd is known to associate with Fe(III) (oxyhydr)oxides in pH-neutral to slightly acidic soils, though it is not well understood how the interrelation of Fe and Cd changes under Fe(III)-reducing conditions. Therefore, we investigated how the mobility of Cd changes when a Cd-bearing soil is faced with organic carbon input and reducing conditions. Using fatty acid profiles and quantitative PCR, we found that both fermenting and Fe(III)-reducing bacteria were stimulated by organic carbon-rich conditions, leading to significant Fe(III) reduction. The reduction of Fe(III) minerals was accompanied by increasing soil pH, increasing dissolved inorganic carbon, and decreasing Cd mobility. SEM-EDX mapping of soil particles showed that a minor fraction of Cd was transferred to Ca- and S-bearing minerals, probably carbonates and sulfides. Most of the Cd, however, correlated with a secondary iron mineral phase that was formed during microbial Fe(III) mineral reduction and contained mostly Fe, suggesting an iron oxide mineral such as magnetite (Fe_3O_4). Our data thus provide evidence that secondary Fe(II) and Fe(II)/Fe(III) mixed minerals could be a sink for Cd in soils under reducing conditions, thus decreasing the mobility of Cd in the soil.

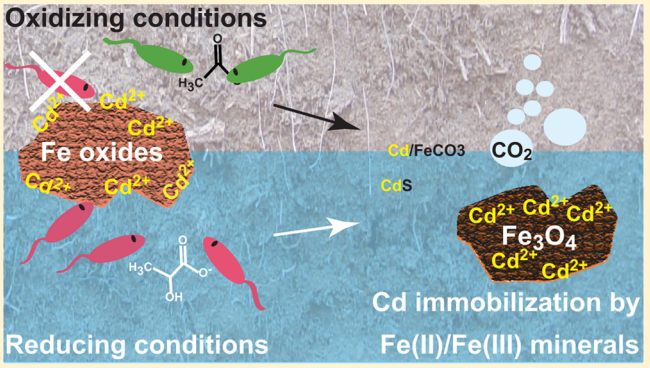

INTRODUCTION

Cadmium (Cd) is widely distributed in agricultural soils[1] and enters the food chain through crops,[2−4] thus threatening human health. Long-term Cd exposure causes malfunctioning of the kidneys and liver, bone degeneration, and cancer.[2] Even though Cd input into agricultural soils via atmospheric deposition, fertilizer use, and manure application has decreased in the past years,[2] elevated concentrations are still present as Cd persists in soils.[2,5] The main fraction of Cd in soils is sorbed to soil particles[6−8] or complexed by organic compounds[9,10] and biomass[11] and can be mobilized from mineral surfaces by competing divalent ions.[12,13] A substantial amount of Cd in agricultural soil is bioavailable to crops, and therefore understanding and assessing factors that influence Cd mobility is of major importance.

Cd associates with clays, Fe oxides, organic matter, sulfides, and carbonates in a pH-dependent manner.[8,13,14] In alkaline soils, Cd not only sorbs to carbonate minerals but can also be part of their crystal structure.[15] Mixed cation carbonate phases with the two mineralogical end members calcite [$CaCO_3$] and otavite [$CdCO_3$] are common.[16] However, most agricultural soils have a pH from 5.0 to 7.5 with carbonates becoming less important but Fe(III) (oxyhydr)oxides and clay minerals being relevant for the mobility of Cd. Sorption of Cd to different Fe(III) (oxyhydr)oxides has been investigated before.[7,17−20] Cd forms either inner-sphere complexes[20] or is bridged to the mineral surface via negatively charged organic molecules.[9] Francis and Dodge found that Cd is more mineral-integrated than surface-bound, since hardly any Cd was retrieved from the exchangeable fraction of goethite minerals,[21] supported by other studies that have shown that Cd was stoichiometrically coprecipitated with Fe(III) (oxyhydr)oxides.[21−23]

The mobility of mineral-associated contaminants is altered during biotic and abiotic Fe redox reactions that form, transform, and dissolve Fe minerals.[12,24−26] Fe(III) (oxyhydr)-

Received: August 2, 2013
Revised: October 29, 2013
Accepted: November 6, 2013
Published: November 6, 2013

oxides are formed during chemical or microbiological oxidation of Fe(II) at circumneutral pH.[12,27] Different Fe(III) oxyhydroxides such as goethite, ferrihydrite, and lepidocrocite form depending on the geochemical conditions.[28,29] The identity of the Fe minerals formed not only affects the type, amount, and binding strength of adsorbing contaminants but also their mobility during microbial Fe(III) reduction.[24,30] In anoxic environments, Fe(III) (oxyhydr)oxides are reduced and dissolved during microbial Fe(III) reduction, thereby releasing associated contaminants.[24,31] However, the formed aqueous Fe^{2+} might react with excess Fe(III) minerals forming mixed-valent Fe(II)/Fe(III) minerals like green rust and magnetite ($Fe^{II}Fe^{III}_2O_4$) or precipitate as Fe(II) phases (e.g., siderite or vivianite).[32−35] The formation of secondary Fe minerals can resequester contaminants by sorption or coprecipitation.[24,30] Changes in mobility of metal(loid)s (Cr, U, As, and others) during microbial Fe(III) reduction have been observed[36−39] and are most prominently discussed for arsenic in Southeast Asia.[40,41] Cd is also associated with Fe minerals, and it has been shown before that in slightly acidic to pH-neutral soils, Cd is mobilized as a consequence of Fe mineral dissolution.[42] However, prolonged reducing conditions caused pH changes and resulted in a net-immobilization of Cd.[42,43] The processes occurring at different stages of Fe(III) reduction, the minerals involved, and whether the formation of secondary Fe minerals influences Cd mobility have not been investigated in detail yet.

Microbial Fe(III) reduction requires anoxic conditions and an electron donor (e.g., organic matter),[44] conditions which are met in agricultural soils during rainfall, flooding, and runoff. Burkhardt et al. have demonstrated the presence of Fe(III)-reducing fermenters and *Geobacter* in anoxic enrichments of Cd-amended soil suspensions.[45] To our knowledge, correlations between Cd mobility and changes in redox conditions, pH, Fe mineralogy, and Fe speciation have been observed in previous studies but have not been analyzed in combination with a quantitative assessment of the presence and activity of the physiological groups of Fe(III) reducing bacteria in the same environment.

The objective of this study therefore was to investigate how C bioavailability, redox conditions, and microbial Fe(III) reduction in a Cd-bearing soil influence Cd mobility. In soil microcosms, the water filled pore space (WFPS) was varied to create either oxidizing or reducing conditions. Lactate and acetate were amended as carbon sources to enhance metabolic activity. Changes in Cd mobility over time were correlated to Fe mineralogy and speciation, soil geochemistry, and 16S rRNA gene copy numbers of total *Bacteria* and *Geobacter* spp.-type Fe(III)-reducers.

MATERIALS AND METHODS

Soil Characterization. Soil was sampled in April 2012 from the field site in Stutenkamm, Germany (N50,412073, E11,554942), which contains approximately 1.1 μg of Cd g^{-1} of dry soil of geogenic origin (Table S1). The soil was dried at room temperature, sieved (2 mm), stored in the dark at 4 °C, and characterized with respect to grain size by sieving. The soil water content was quantified by drying (105 °C). Soil pH was determined after 24 h of incubation with 0.01 M $CaCl_2$ at a liquid/soil ratio of 2.5:1. Total inorganic carbon (TIC) and total organic carbon (TOC) were determined from 60 °C dried soil samples. For TIC quantification, dried soil samples were acidified with HCl until carbonates were released followed by NaOH neutralization. TIC was calculated from the amount of NaOH used. TOC was quantified from decalcified samples. Extractable organic carbon (OC) and inorganic carbon (IC) were determined in duplicates by extracting 5 g of soil with 40 mL of 0.5 M K_2SO_4 (1 h, 25 °C, 150 rpm) and filtering the soil extracts through Whatman 1573 1/2 cellulose filters, followed by filtration through 0.45 μm syringe filters (Millex HA filter, Millipore). For sequential Fe extraction, two times 0.5 g of soil were weighed into glass vials and extracted sequentially with anoxic 0.5 M HCl (1 h, 25 °C, 150 rpm) and 6 M anoxic HCl (24 h, 70 °C) in the absence of O_2 to prevent Fe(II) oxidation.[46] Samples were diluted in 1 M HCl and stored anoxically until Fe speciation analysis. In order to quantify heavy metals associated with poorly crystalline minerals, soil samples of 1 g were extracted in duplicate with 10 mL of 0.1 M HCl (0.5 h, 25 °C, 150 rpm),[47] followed by filtration through Whatman #1 filters, stabilization with 1 mL of 65% HNO_3, and analysis by ICP-MS and ICP-OES (see below). Total cation, P, and S contents were extracted in triplicate (0.25 g of soil, 1.8 mL of 37% HCl, 0.6 mL of 65% HNO_3) at 25 °C for 20 h, followed by 60 °C for 2 h, 75 °C for 2 h, and 100 °C for 5 h. Extracts were filled up to 10 mL with deionized water and filtered through Whatman #1 filters.

Experimental Setup. Experiments were set up in duplicate for each experimental condition and time point by weighing 45 g of air-dried soil into 58 mL sterile serum bottles. Bottles were closed with butyl stoppers and transferred to an anoxic chamber (N_2), in order to extract the different Fe redox species according to Porsch and Kappler.[46] To create different soil redox conditions, the WFPS was adjusted to either 70 or 100% by adding anoxic, sterile deionized water (10.5 or 30 mL; Millipore). For selected setups, the OC content of the soil (21.0 ± 0.3 mg g^{-1} soil) was increased by adding 2.5 mL of an anoxic stock solution containing 1 M Na-lactate and Na-acetate each, followed by the addition of 8 or 27.5 mL of deionized water to obtain a WFPS of 70 or 100%. The addition of lactate/acetate corresponded to 3.3 mg of extra OC g^{-1} of soil, resulting in a total OC content of approximately 24.3 mg g^{-1} of dry soil in the organic acid-amended microcosms. Closed bottles were shaken for homogeneous distribution of the water and organic acids. Homogeneity was verified by determining the water and 0.5 M K_2SO_4-extractable OC content in samples from different locations of several bottles (data not shown). The bottles were covered loosely with aluminum caps and incubated oxically without shaking at 22 °C in the dark. Oxygen entering the bottles rendered the 70% WFPS setups oxic. At 100% WFPS, the oxygen diffusing slowly into the water-saturated soil is consumed rapidly by aerobic respiration, leaving these setups mostly anoxic.[48] Sterile deionized water was added weekly to replace the water loss (determined by weighing) due to microbial activity and evaporation.

Sampling. Entire bottles (duplicates) were harvested at each time point (0, 2, and 6 weeks) and additionally after 4 and 11 weeks for the 100% WFPS setup amended with organic acids. For sampling, bottles were closed with stoppers. The 100% WFPS bottles were centrifuged (13 min; 4000*g*). All bottles were transferred into an anoxic chamber, where the supernatant of the 100% WFPS bottles were decanted. A 2-mL aliquot was centrifuged (13000*g*, 2 min) for analysis of organic acids. The sequential Fe extraction was performed in the glovebox, while samples for other geochemical and microbial characterization were taken outside the glovebox. Approximately 5 g of soil was frozen at −20 °C for molecular biological analysis. As the formation of gas bubbles was observed in the

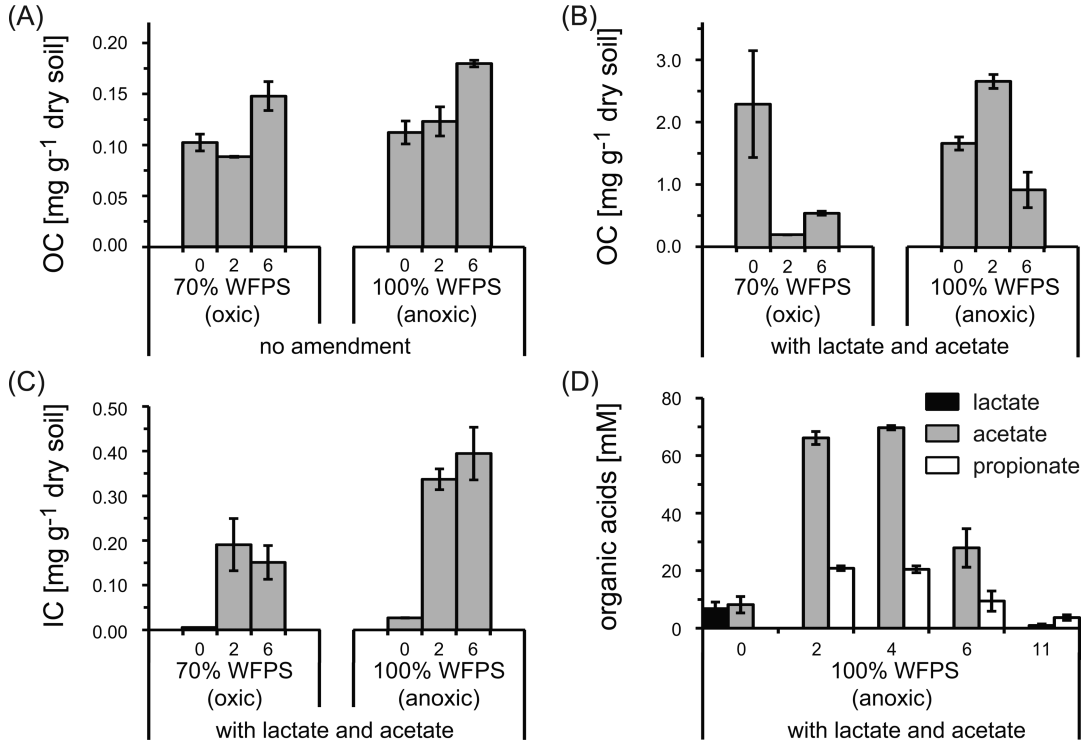

Figure 1. K_2SO_4-extractable OC, IC, and organic acid concentrations during incubation of Stutenkamm soil with either 70 or 100% WFPS in the presence or absence of amended lactate and acetate. OC and IC are presented per gram of dry soil for time points 0, 2, and 6 weeks (mean ± range, $n = 2$). Extractable OC is shown for microcosms without amendment (a) and for microcosms with amended lactate and acetate (b). Extractable IC is shown for microcosms with amended lactate and acetate (c). Organic acid analysis of the supernatant for the 100% WFPS microcosms with additional lactate and acetate after 0, 2, 4, 6, and 11 weeks of incubation (d). Lactate, black; acetate, gray; propionate, white; other organic acids were below the detection limit and are not shown (mean ± standard deviation, $n = 2$).

100% WFPS microcosms, additional bottles were closed with butyl stoppers, shaken, centrifuged, and analyzed for methane.

Molecular Biology Methods. DNA extraction and qPCR quantification of total *Bacteria* and *Geobacter* spp. are described in detail in the Supporting Information.

Analytical Methods. Total Fe(II) and Fe(III) were quantified in triplicate using the ferrozine assay.[49] Samples for total ion analysis were extracted with 0.1 M HCl, diluted in 2% HNO_3 and analyzed by ICP-OES (PerkinElmer Optima 5300 DV). Samples for determining total ion concentrations were diluted 2-fold in MQ water and measured with ICP-MS (Thermo-Fisher XSeries2) and ICP-OES. TIC, TOC, and K_2SO_4-extractable OC and IC were determined in duplicate as described above for the original soil (VarioEL T/N analyzer and HighTOC analyzer, Elementar, Hanau, Germany). Organic acids in the supernatant of the 100% WFPS setup were identified and quantified using HPLC (Shimadzu LC-10AVP, Aminex HPX-87H column, 5 mM H_2SO_4 eluent, flow rate 0.6 mL min^{-1}). Acetate, lactate, formate, and pyruvate were analyzed with a refractive index detector (RID 10A, Shimadzu), while butyrate and propionate were quantified by UV absorption (SPD-M 10A VP, Shimadzu). Methane was identified by gas chromatography (Varian CP-3800 Agilent, USA). For X-ray diffraction (XRD), vacuum-dried soil was ground in an agate mortar in an anoxic glovebox and transferred onto a silicon wafer. Each measurement was done oxically between 5 and 75° within 3−5 min to minimize exposure to O_2 using a bulk-XRD (Bruker D8 Discover XRD instrument, Bruker AXS GmbH, Germany) equipped with a Co Kα source. Spatially resolved elemental maps were acquired using SEM-EDX mapping and evaluated for spatial correlation using ImageJ[50] as described in the Supporting Information.

RESULTS

Characterization of Stutenkamm Soil before and during Incubation. The soil used for the present study from the field site in Stutenkamm is sandy with approximately 4% clays and silts and 2% OC and contained ca. 12% Fe (w/w; Table S1). It also contained Cd (1.1 μg g^{-1} of dry soil), Ca (4 mg g^{-1} of dry soil), S (250 μg g^{-1} of dry soil), and Mn (1 mg g^{-1} of dry soil; Table S1). During the incubation of lactate/acetate-amended anoxic soil microcosms (100% WFPS), the water phase turned turbid with a brownish color accompanied by a smell characteristic for fermentation processes. Additionally, gas bubbles were observed at the soil−glass interface, and the presence of methane was confirmed by gas chromatography (data not shown). Methane was below the detection limit in the gas phase of oxic (70% WFPS) and noncarbon-amended anoxic (100% WFPS) microcosms.

The initial pH of the soil was approximately 6.3 for setups without lactate/acetate and 6.45 for lactate/acetate-amended microcosms (Table S2). In the absence of amended organic acids, the pH did not change significantly during incubation of the oxic microcosms, while it slightly increased to 6.7 in the anoxic microcosms within six weeks. In lactate/acetate-amended microcosms, the pH of the oxic soil increased to approximately 8. In the anoxic setup, the pH first dropped slightly to 6.3, before it steadily increased to approximately 7.6 toward week 11.

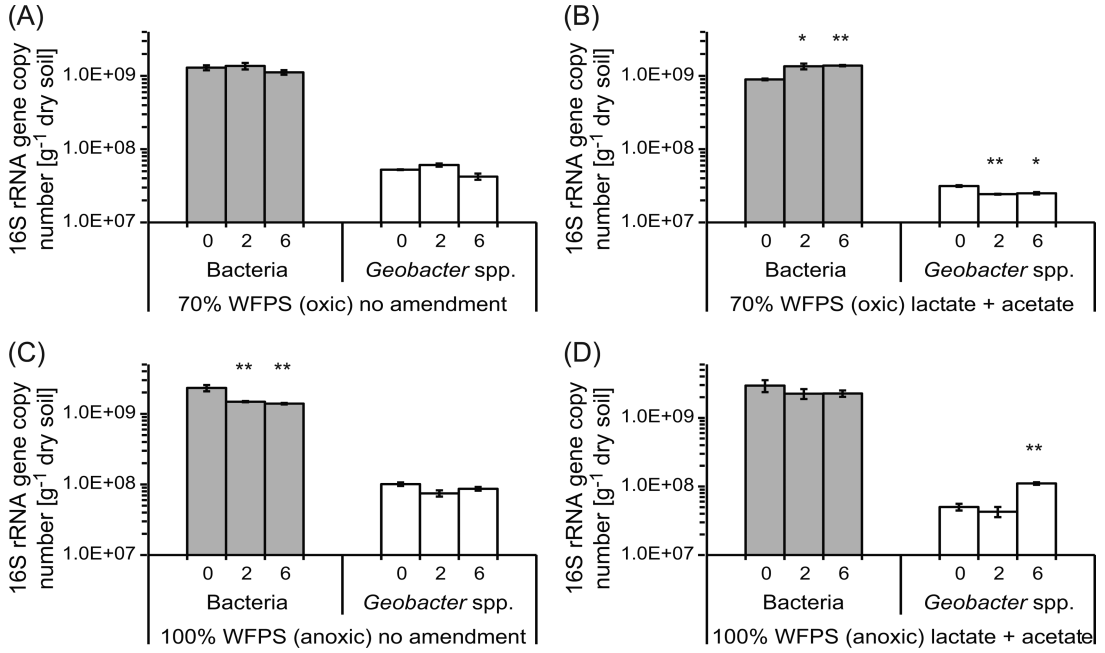

Figure 2. Number of total *Bacteria* (gray) and *Geobacter* spp. (white) per gram of dry soil present during the incubation of Stutenkamm soil. 70% WFPS microcosms in the absence (a) and presence of additional acetate and lactate (b) and 100% WFPS microcosms in the absence (c) and presence of additional acetate and lactate (d). 16S rRNA gene copy numbers were quantified after 0, 2, and 6 weeks. Asterisks indicate whether the mean of the gene copy numbers at the beginning of the experiment are significantly different from the mean after incubation using the unpaired *t* test at a 95% confidence interval (* for $P < 0.05$, ** for $P < 0.01$, and *** for $P < 0.001$). Mean ± range, $n = 2$.

Changes in (In)Organic Carbon and Organic Acid Concentrations during Incubation. Microcosms without lactate/acetate amendment contained initially ca. 0.1 mg g^{-1} of dry soil K_2SO_4-extractable OC, which increased by 0.05−0.1 mg g^{-1} of dry soil in both the oxic and anoxic setups within six weeks of incubation (Figure 1a). In the lactate/acetate-amended microcosms, approximately 2 mg of K_2SO_4-extractable OC was initially present per gram of dry soil (Figure 1b). In the oxic setup, the extractable OC decreased below 0.5 mg g^{-1} of dry soil already within two weeks, while in the anoxic microcosms, the extractable OC first increased to 2.6 ± 0.1 mg g^{-1} of dry soil and then dropped to 0.9 ± 0.3 mg g^{-1} of dry soil within six weeks.

Lactate/acetate-amended microcosms contained initially less than 0.03 mg K_2SO_4-extractable IC, which increased to 0.19 ± 0.06 and 0.34 ± 0.02 mg IC g^{-1} of dry soil in oxic and anoxic setups within two weeks, respectively (Figure 1c). Extractable IC in microcosms without added lactate/acetate remained below the quantification limit throughout the experiment (data not shown). The soil TIC content (3.1 ± 0.5% w/w, Table S1) did not change significantly in any setup before, during, and after incubation (data not shown).

To determine the fate of the added acetate and lactate in the anoxic microcosms, organic acids were quantified in the water phase (Figure 1d). Initially equimolar concentrations (approximately 7.5 mM) of lactate and acetate were determined in the supernatant (Figure 1d). Within two weeks, lactate disappeared completely, while acetate concentrations increased 10-fold and approximately 20 mM propionate was present. Both acetate and propionate remained constant for another two weeks and decreased after 11 weeks to levels below the quantification limit (0.25 mM). No formate, pyruvate, and butyrate were detected throughout the experiment (data not shown).

Cell Numbers of Total Bacteria and *Geobacter* spp. 16S rRNA Gene Targeted. Quantitative PCR was used to estimate total *Bacteria* and *Geobacter* spp. cell numbers. Initially, total *Bacteria* accounted for approximately 10^9 16S rRNA gene copies g^{-1} of dry soil in all setups (Figure 2). The number of *Geobacter* spp. cells was approximately 100-fold lower than the number of total *Bacteria*. Over a period of six weeks, 16S rRNA gene copy numbers of total *Bacteria* and *Geobacter* spp. did not change significantly in nonamended oxic microcosms (Figure 2a). In lactate/acetate-amended oxic microcosms, total 16S rRNA gene copy numbers increased from $9.0 \times 10^8 \pm 2.3 \times 10^7$ to $1.4 \times 10^9 \pm 2.8 \times 10^7$ cells $g^{-1}$of dry soil, while *Geobacter* spp. decreased from $3.2 \times 10^7 \pm 8.3 \times 10^5$ to $2.5 \times 10^7 \pm 9.5 \times 10^5$ cells g^{-1} of dry soil (Figure 2b). For the anoxic setup without lactate/acetate, total 16S rRNA gene copy numbers decreased from $2.3 \times 10^9 \pm 2.3 \times 10^8$ to $1.4 \times 10^9 \pm 3.7 \times 10^7$ cells g^{-1} of dry soil, while *Geobacter* spp. remained constant (Figure 2c). Total 16S rRNA gene copy numbers did not change in the lactate/acetate-amended anoxic microcosms in contrast to the *Geobacter* spp. 16S rRNA gene copy numbers, which increased from $5.0 \times 10^7 \pm 5.6 \times 10^6$ to $1.1 \times 10^8 \pm 4.8 \times 10^6$ cells g^{-1} of dry soil after six weeks (Figure 2d).

Changes in Fe and Cd Geochemistry during Incubation. In order to determine the effect of microbial Fe(III) reduction on Cd mobility, we followed the speciation and quantity of extractable Fe and Cd (Figure 3). Both 0.5 M HCl- and 6 M HCl-extractable Fe(II) and Fe(III) were quantified to account for poorly crystalline and crystalline Fe fractions, respectively (Figure 3a−d).[46,51,52] Initially, 6−10% of the total Fe in the soil belonged to the poorly crystalline Fe fraction (8−9 mg Fe g^{-1} of dry soil; Figure 3a,b), which increased to approximately 20% during Fe(III) reduction in anoxic setups with lactate/acetate (Figure 3b). No change in

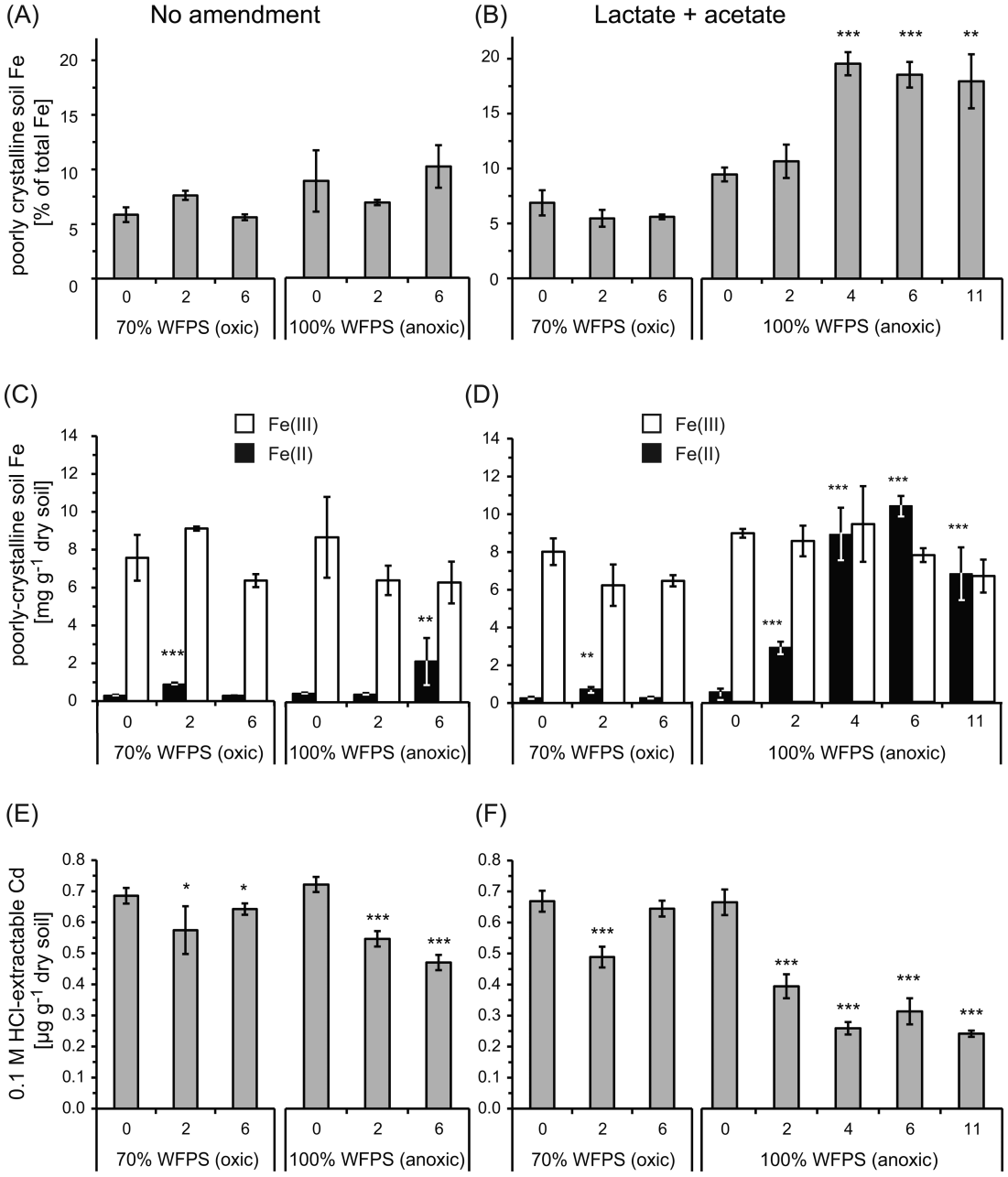

Figure 3. Amount of poorly crystalline Fe (a,b), poorly crystalline Fe(II) and Fe(III) (c,d), and poorly crystalline-mineral-associated Cd (e,f), per gram of dry soil during incubation of Stutenkamm soil with either 70 or 100% WFPS in the presence (b,d,f) or absence (a,c,e) of additional lactate and acetate. Poorly crystalline Fe (a,b, gray) is given in % of total Fe. Poorly crystalline Fe(II) (black) and Fe(III) (white) (c,d) are given in mg g^{-1} of dry soil. Poorly crystalline-mineral-associated Cd (e,f, gray) was extracted with 0.1 M HCl and is given in μg g^{-1} of dry soil. Microcosms without additional organic acids were analyzed after 0, 2, and 6 weeks of incubation, while 100% WFPS microcosms with supplemented lactate and acetate were analyzed after 0, 2, 4, 6, and 11 weeks of incubation. Asterisks indicate whether the mean of the values (Fe(II) and Cd) at the beginning of the experiment is significantly different from the mean after incubation using the unpaired *t* test at a 95% confidence interval (* for $P < 0.05$, ** for $P < 0.01$, and *** for $P < 0.001$). Mean ± standard deviation, $n = 4$.

the amount of poorly crystalline Fe was detected in any other setup.

When analyzing the Fe redox speciation, we found that in anoxic microcosms with additional lactate/acetate, Fe(II) increased from 0.5 ± 0.2 to 2.9 ± 0.3 mg g^{-1} of dry soil after two weeks and reached its maximum after six weeks with 10.4 ± 0.5 mg g^{-1} of dry soil (Figure 3d). In anoxic microcosms without additional organic acids, poorly crystalline Fe(II) increased from 0.4 ± 0.1 to 2.2 ± 1.2 mg Fe(II) g^{-1} of dry soil only after six weeks (Figure 3c). In the oxic microcosms, Fe(II) increased within the first two weeks from 0.28 ± 0.01 to 0.88 ± 0.10 and to 0.73 ± 0.12 mg Fe(II) g^{-1} of dry soil in the nonamended and organic-acid-amended setups, respectively, and decreased thereafter (Figure 3c,d).

The initial amount of 0.1 M HCl-extractable Cd was between 0.66 and 0.72 μg g^{-1} of dry soil (Figure 3e,f). In anoxic microcosms with amended lactate/acetate, HCl-extractable Cd decreased to 0.26 ± 0.02 μg g^{-1} of dry soil after four weeks and remained at this concentration throughout 11 weeks (Figure 3f). In anoxic setups without additional organic acids, the HCl-

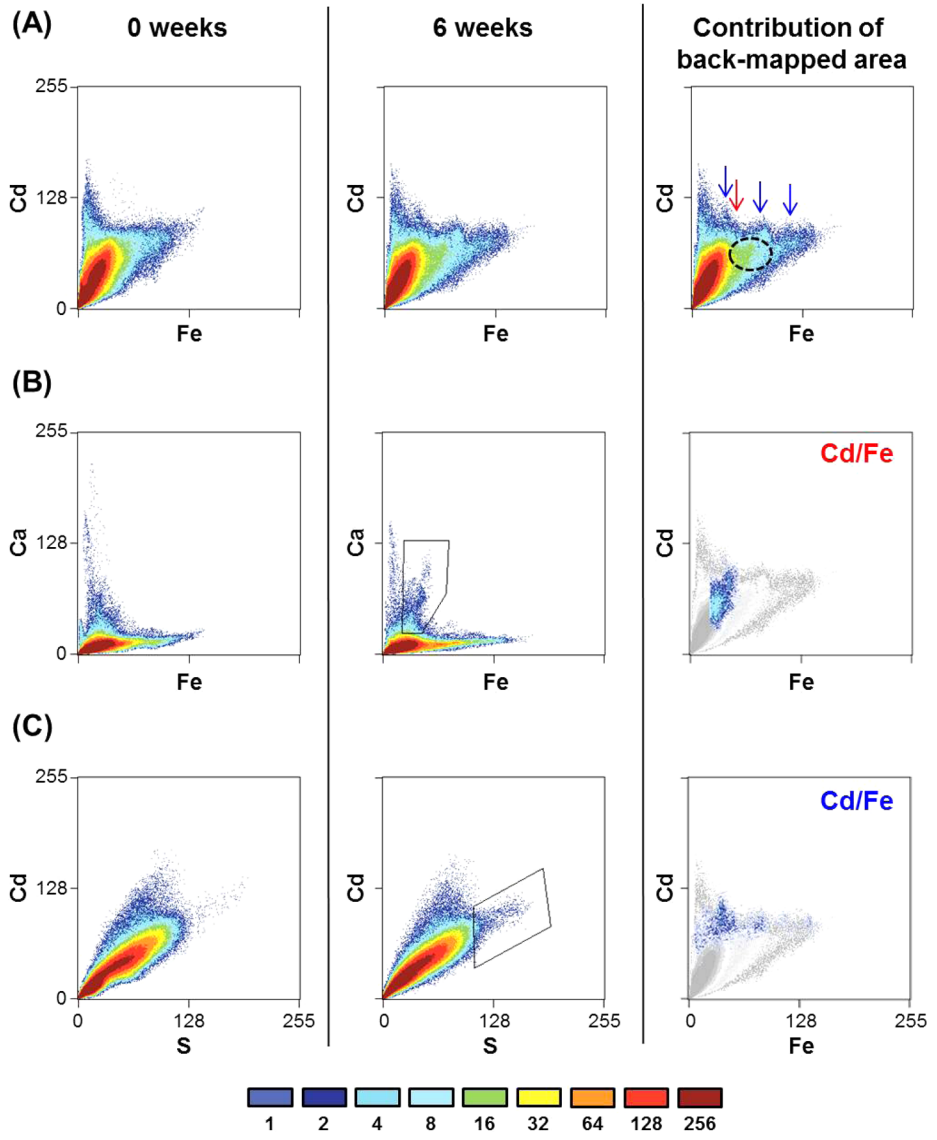

Figure 4. Scatterplots of EDX maps representing different elements in the 100% WFPS Stutenkamm soil with amended lactate and acetate during incubation. For each pixel position, a data point is created by the gray values in two images, representing the local concentration of a certain element, serving as coordinates. The number of pixels with a certain combination of contents of the two respective elements is indicated in the color scheme at the bottom. Horizontal and vertical clusters in the 2D histogram indicate regions on the sample wherein one element is independent of the other. Clusters with a positive slope, in contrast, represent regions on the sample wherein both elements are associated with each other (i.e., correlate). Cd is plotted versus Fe (a), Ca versus Fe (b), and Cd versus S (c). The difference in element correlation was determined at the start of the experiment (0 weeks, left column) and after six weeks of incubation (6 weeks, middle column). Different clusters of particularly high correlations that appeared after six weeks of incubation were selected in the maps to create a mask of the corresponding pixels (backmapping). The contribution of these areas to the Cd/Fe scatterplots is shown in the right-middle and -bottom images, which indicate corresponding correlations between three elements. The red and blue arrows indicate the contribution of Ca and S, respectively, in the Cd/Fe scatterplot, and the area highlighted with a black circle does not correlate with any other element other than Cd and Fe.

extractable Cd decreased to 0.47 ± 0.02 μg g^{-1} of dry soil after six weeks (Figure 3e). In the nonamended and lactate/acetate-amended oxic microcosms, the amount of HCl-extractable Cd decreased in the first two weeks to 0.57 ± 0.08 and 0.49 ± 0.03 μg of Cd g^{-1} of dry soil and increased again after six weeks to 0.64 ± 0.02 and 0.65 ± 0.03 μg of Cd g^{-1} of dry soil, respectively. Total Cd did not change over the course of the experiment (data not shown).

Changes in Fe Mineralogy during Incubation. Evaluation of the soil Fe mineralogy by sequential Fe extraction showed that before incubation the soil contained approximately 7% poorly crystalline Fe with mainly Fe(III). After incubation, anoxic, carbon-amended soil microcosms contained ca. 10% poorly crystalline Fe(II)-containing minerals (e.g., siderite and vivianite) and ca. 8% poorly crystalline Fe(III) minerals (e.g., ferrihydrite) (Figure 3b,d). Extraction of these anoxic microcosms after incubation using 6 M HCl indicated the presence of ca. 55% crystalline Fe(III) minerals (e.g., goethite or hematite) and ca. 27% crystalline Fe(II)-containing minerals. Mixed-valent Fe(II)/Fe(III) mineral phases (e.g., magnetite) could be present in both fractions. Unfortunately, XRD analyses did not reveal the identity of the Fe minerals since the diffraction patterns were dominated by clays and silicates (data not shown).

Cd Distribution and Elemental Correlations in Soil Aggregates. Since the presence of minor mineral phases in the soil was superimposed by dominating silicate and clay minerals in XRD, and since the identification of changes in the Fe mineralogy using Mössbauer spectroscopy was not feasible, as a change in Fe mineralogy of at least several % of the total Fe in the soil is necessary for reliable detection, we analyzed elemental correlations using spatially resolved elemental distribution maps (EDX). This allowed for the simultaneous analysis of thousands of individual soil aggregates regarding their elemental composition. An exemplary SEM image of a soil sample and the corresponding element maps are shown in Figure S1. The 2D histograms derived from the EDX elemental maps visualize correlations of Cd with Fe, Ca with Fe, and Cd with S. The 2D histograms were determined in lactate/acetate-amended 100% WFPS before and after 6 weeks of incubation (Figure 4).

Initially, a major fraction of Cd correlated clearly with Fe (Figure 4a, left). This is indicated by a high number of pixels along a slope or the diagonal of the 2D histogram, which is equivalent to a high number of particles with Cd concentrations that vary correlatively with the concentrations of another element. After six weeks of incubation, the main fraction of Cd still correlated with Fe; however, the distribution pattern had changed (Figure 4a, center). A new Fe/Cd cluster appeared after six weeks that showed a high pixel count, indicating that a large fraction of Cd was associated with Fe (Figure 4a, right, green region circled in black). This region did not correlate with any other element (i.e., vertical and/or horizontal distribution patterns in the 2D histogram). Additionally, two more very minor (low pixel) Cd fractions were detected that correlated with different Fe fractions. One was located in the lower Fe region (Figure 4a right, red arrow) and correlated with Ca (Figure 4b), though the extent of the Ca−Cd correlation was minor throughout the experiment (Figure S2). Another minor Cd region correlated to a broader Fe region (Figure 4a right, blue arrows) and colocalized with S (Figure 4c).

Backmapping the regions where Cd initially did not correlate with Fe to other elemental plots showed that Cd correlated highly with Al. The correlation between Al and Cd increased slightly after six weeks (Figure S3). Cd also correlated initially to a minor extent with Mn but not anymore after six weeks of incubation (Figure S3d). Scatterplots of Cd, Mg, and K did not show any significant changes in correlations between these elements during incubation (Figure S3).

DISCUSSION

Stimulation of Microorganisms in Soil Microcosms under Different Incubation Conditions. The incubation of Cd-bearing soil under oxidizing (70% WFPS) and reducing (100% WFPS) conditions with or without lactate/acetate amendment stimulated different physiological groups of microorganisms to metabolize and/or grow in the individual microcosms. Under oxidizing conditions and in the absence of lactate/acetate, aerobic bacteria were expected to utilize the low amount of bioavailable carbon present.[53] However, if growth is taken as an indicator for activity, these microorganisms were not very active in the microcosms as evidenced by constant 16S rRNA gene copy numbers and stable extractable IC concentrations within six weeks of incubation. Extractable OC increased slightly, probably due to a slow mobilization of OC from non-K_2SO_4-extractable OC pools and/or by cell lysis and release of cellular organic molecules.[54] In contrast, aerobic microbes in lactate/acetate-amended oxic microcosms used the added organic carbon for growth, as evidenced by lower OC concentrations and increased 16S rRNA gene copy numbers after incubation. Decreasing *Geobacter* spp. 16S rRNA gene copy numbers showed that the oxic incubation conditions were not favorable for anaerobic Fe(III) reducers.

In microcosms incubated under reducing conditions without lactate/acetate addition, Fe(III) reduction occurred as indicated by increasing Fe(II) concentrations over six weeks of incubation. Aerobic bacteria were probably not active under O_2-limited conditions.[53] The conditions applied in these microcosms (anoxic, no C amendment) were not favorable for significant cell growth, as evidenced by decreasing total *Bacteria* 16S rRNA gene copy numbers. However, cell lysis can cause an increase in extractable OC, allowing fermenters or Fe(III) reducers to perform direct or indirect Fe(III) reduction.[55] It was shown previously that Fe(III) reducers do not compete successfully with fermenters at low concentrations of bioavailable organic carbon,[55] supporting our results of decreasing 16S rRNA gene copy numbers of *Geobacter* spp. in the anoxic setups without lactate/acetate amendment.

In contrast, the addition of bioavailable carbon, i.e. lactate/acetate, to reducing microcosms enhanced the growth of Fe(III)-reducing bacteria as indicated by an increase in *Geobacter* spp. 16S rRNA gene copy numbers. Fermenters were also active as evidenced by the formation of the typical fermentation products acetate and propionate in accordance with increasing extractable OC and IC after the first two weeks of incubation. The newly formed and initially present acetate can be used by methanogens explaining the presence of methane in lactate/acetate-amended microcosms. Additionally, acetate can be used as an electron donor by Fe(III)-reducing *Geobacter* spp.,[44] evidenced by increasing *Geobacter* spp. 16S rRNA gene copy numbers. Fe(III) reducers were also able to reduce more crystalline Fe(III) phases[56] as the fraction of poorly crystalline Fe increased in anoxic microcosms amended with lactate/acetate.

Alkalization during Organic Carbon Oxidation and Consequences for Carbonate Mineral Formation. During incubation of organic carbon-rich soil, OC is metabolized via oxidation or fermentation to HCO_3^-, which usually causes an initial drop in pH as protons are released.[53] However, CO_2 is expected to degas from solution, releasing hydroxyl ions and explaining the observed overall increase in pH in our microcosms. In the lactate/acetate-amended oxic microcosms, CO_2 was produced rapidly, and the water phase was too little to take up all the formed HCO_3^-, causing CO_2 to degas and the pH to rise even more quickly.[57] In contrast, fermentation is slower and produces intermediate short-chained organic acids and less CO_2,[53] which is reflected by a slower and lower increase in pH in the lactate/acetate-amended anoxic microcosms.[53] Under these conditions, Fe(III) oxyhydroxide mineral reduction releases hydroxyl ions that react with the protons released during fermentative production of CO_2, which dissolves as HCO_3^- in the water phase. In anoxic microcosms without lactate/acetate, the pH of the soil only increased by 0.4 units, as mainly Fe(III) reduction occurred. An increasing pH under reducing conditions in soils was also observed previously.[58]

Because of the high increase in pH and IC, we expected the precipitation of carbonate minerals, which are considered a main, but instable sink for Cd.[59] Mixed carbonate mineral

phases including calcite [$CaCO_3$], magnesite [$MgCO_3$], siderite [$FeCO_3$], and otavite [$CdCO_3$] could potentially form in Stutenkamm soil as all of the necessary cations are present (Table S1). However, the amount of these minerals was too low to be detected by XRD or by acidic extractions, suggesting that carbonate was not an important mineral for Cd sequestration.

Minor Association of Cd with Carbonate and Sulfur under Reducing Conditions. During anoxic incubation of Stutenkamm soil with lactate/acetate amendment, Cd concentrations decreased in the 0.1-M-HCl-extractable metal fraction. This shows that Cd was sequestered in soil mineral phases that were not soluble in 0.1 M HCl. The immobilization of Cd under reducing conditions has been attributed to sequestration by carbonates and sulfides.[43,58] We conclude that in our study carbonates play a minor role for the sequestration of Cd under reducing conditions as supported by TIC analyses and the weak correlation of Ca and Cd observed in the EDX maps. Nevertheless, a minor increase in the correlation of Cd, Ca, and Fe during six weeks of incubation showed that some Cd was transferred to a Ca and Fe rich phase that could potentially be a mixture of Ca- and Fe-carbonates.

Reducing conditions not only stimulated Fe(III) reduction but also allowed the reduction of sulfate to sulfide by sulfate-reducing microbes.[53,60] At a pH above 7 as present in the anoxic lactate-/acetate-amended microcosms, hydrogen sulfide (H_2S, pK_a 6.9) dissociates into HS^-,[53,60] which reacts with Cd^{2+}, forming CdS.[43,58,61] Such a process is indicated by the EDX maps, wherein sulfur correlated weakly with Cd after six weeks of reducing conditions. However, although the correlation between Cd and S within this cluster was present, we expect only minor amounts of Cd to be bound to S since this cluster only consisted of a limited number of pixels. In summary, our results show that the immobilized Cd is associated to a minor extent with carbonate and sulfide minerals and the formation of other minerals must be responsible for Cd immobilization.

Redistribution of Cd to Crystalline Mineral Phases. A small fraction of Cd correlated initially with Mn, potentially Mn oxides (Figure S3). Under anoxic conditions, Mn(IV) oxides are microbially reduced similar to Fe(III) oxyhydroxides[44] releasing associated Cd as evidenced by the absence of a correlation in the Cd and Mn elemental maps after six weeks. This suggests that a small pool of Cd was released from Mn oxides and that the formed Mn(II) phases did not bind Cd.

Prior to incubation, Cd was mainly associated with Fe and Al, suggesting that Cd was partly sorbed or coprecipitated with Fe(III) minerals and clays. During oxic incubation, 9% Fe(II) of poorly crystalline Fe was formed within two weeks, indicating the activity of Fe(III) reducers that thrive in anoxic soil microenvironments.[58] The increase in Fe(II) correlated with neither an increase in pH nor carbonate formation, but with a decrease in extractable Cd. This indicates that shifts in Cd mobility are directly influenced by Fe(III) reduction and the formation of new Fe mineral phases as postulated among others by Zhang et al.[62]

After six weeks of anoxic incubation, the correlation of Cd and Al had slightly increased, suggesting that mobile Cd^{2+} ions diffused into the layers of swelling clays that are fully submersed in water in these setups.[63] Additionally, in the Cd/Fe 2D histogram, a new cluster appeared (black circle in Figure 4a) that corresponded to pixels wherein Cd correlated with Fe but not with other elements. This suggests that the respective Cd-enriched mineral phase could be an Fe oxide mineral with some incorporated Cd. Although XRD analysis failed to provide evidence for magnetite formation in our microcosms due to the high background of silicates and clays, magnetite is a potential candidate for an Fe oxide formed in our anoxic, carbon-amended microcosms, since this mixed-valent Fe(II)/Fe(III) mineral often forms during Fe(III) reduction.[12,33−35,64]

Magnetite was shown to sorb Cd^{2+} [12,65] and incorporate Cd^{2+} in its mineral structure.[22,23] According to the Fe extraction data, a minimum amount of 40 mg total Fe(II) g^{-1} of dry soil was present after six weeks of anoxic incubation with lactate/acetate (data not shown). A theoretical estimation assuming that half of that Fe(II) (20 mg, 0.36 mmol) is present in the form of magnetite suggests that approximately 83 mg of magnetite could form per gram of dry soil, since stoichiometric magnetite contains 1 mol of Fe(II) per mol of magnetite. Assuming further that one Cd^{2+} ion replaces one tetrahedral Fe(III)[23] in every 100th magnetite unit (equals 3.6 nmol of magnetite, which is the same amount for Fe and hence Cd), we can estimate that approximately 0.4 mg of Cd could have been incorporated into magnetite per gram of dry soil. This is approximately 1000 times more than the amount of Cd that was actually removed from the fraction extractable with 0.1 M HCl and therefore can explain at least a large part of the Cd sequestration during Fe(III) reduction in our anoxic soil microcosms.

Environmental Implications. In the present study, we provide evidence that under reducing conditions the activity of fermenting and Fe(III)-reducing bacteria redistributes Fe-associated Cd into a more stable Fe mineral phase, most probably magnetite, and only to a minor extent into sulfides and carbonates. Magnetite is more stable than Fe(II), Ca(II), and Cd(II) carbonates, which are dissolved easily upon acidification or reoxidation of soils.[12] Nanocrystalline and biogenic magnetite is applied successfully in metal remediation, and current research focuses on environmental applications for magnetite.[65−67] In the present study, we show that secondary Fe-phases formed during microbial reduction of Fe(III) minerals could potentially result in a net immobilization of Cd, removing Cd from the bioavailable fraction of the soil. We suggest to further investigate the redox-cycling of Fe and specifically the role of magnetite in the removal of Cd in soils.

■ ASSOCIATED CONTENT

Ⓢ Supporting Information

Table S1 and S2; Material and Methods S1 and S2; Figures S1, S2, and S3. This material is available free of charge via the Internet at http://pubs.acs.org.

■ AUTHOR INFORMATION

Corresponding Author

*Phone: +49-7071-2974992. Fax: +49-7071-295059. E-mail: andreas.kappler@uni-tuebingen.de.

Notes

The authors declare no competing financial interest.

■ ACKNOWLEDGMENTS

We thank K. Stoegerer, M. Loganathan, J. M. Byrne, E. Struve, S. Flaiz, P. Kuehn, and S. Will for assistance with analytics; P. Ingino for discussion of the SEM-EDX data; H. Schulz for help with SEM; and A. Piepenbrock and T. Borch for discussion and manuscript improvement. This work was supported by a

scholarship from the German Federal Environmental Foundation to E.M.M. and by the Emmy-Noether program of the DFG to M.O. (OB 362/1-1).

REFERENCES

(1) *European Commission-Joint Research Council, land management and natural hazards unit - Cadmium in European agricultural soils*; EU-JRC: Ispra, Italy, 2010.

(2) *United Nations Environment Programme - Final review of scientific information on cadmium*; UN-EP: Nairobi, Kenya, 2010.

(3) Latterell, J. J.; Dowdy, R. H.; Larson, W. E. Correlation of extractable metals and metal uptake of snap beans grown on soil amended with sewage sludge. *J. Environ. Qual.* **1978**, *7* (3), 435−440.

(4) Mench, M. J. Cadmium availability to plants in relation to major long-term changes in agronomy systems. *Agric., Ecosyst. Environ.* **1998**, *67* (2−3), 175−187.

(5) McLean, J. E.; Bledsoe, B. E. *Behavior of metals in soils*; United States Environmental Protection Agency: Washington, DC, 1992; Vol. *14*.

(6) Hickey, M. G.; Kittrick, J. A. Chemical partitioning of cadmium, copper, nickel and zinc in soils and sediments containing high levels of heavy metals. *J. Environ. Qual.* **1984**, *13* (3), 372−376.

(7) Waseem, M.; Mustafa, S.; Naeem, A.; Koper, G. J. M.; Shah, K. H. Cd^{2+} sorption characteristics of iron coated silica. *Desalination* **2011**, *277* (1−3), 221−226.

(8) Tessier, A.; Rapin, F.; Carignan, R. Trace-metals in oxic lake-sediments - possible adsorption onto iron oxyhydroxides. *Geochim. Cosmochim. Acta* **1985**, *49* (1), 183−194.

(9) Tessier, A.; Fortin, D.; Belzile, N.; DeVitre, R. R.; Leppard, G. G. Metal sorption to diagenetic iron and manganese oxyhydroxides and associated organic matter: Narrowing the gap between field and laboratory measurements. *Geochim. Cosmochim. Acta* **1996**, *60* (3), 387−404.

(10) Holm, P. E.; Andersen, B. B. H.; Christensen, T. H. Cadmium solubility in aerobic soils. *Soil Sci. Soc. Am. J.* **1996**, *60* (3), 775−780.

(11) Higham, D. P.; Sadler, P. J.; Scawen, M. D. Cadmium resistant *Pseudomonas putida* synthesizes novel cadmium proteins. *Science (Washington, DC, U. S.)* **1984**, *225* (4666), 1043−1046.

(12) Cornell, R. M.; Schwertmann, U. *The iron oxides: structure, properties, reactions, occurences and uses*, 2nd ed.; Wiley-VCH Verlag GmbH & Co. KGaA: New York, 2003.

(13) Bradl, H. B. Adsorption of heavy metal ions on soils and soils constituents. *J. Colloid Interface Sci.* **2004**, *277* (1), 1−18.

(14) Arao, T.; Kawasaki, A.; Baba, K.; Mori, S.; Matsumoto, S. Effects of water management on cadmium and arsenic accumulation and dimethylarsinic acid concentrations in Japanese Rice. *Environ. Sci. Technol.* **2009**, *43* (24), 9361−9367.

(15) Buekers, J.; Van Laer, L.; Amery, F.; Van Buggenhout, S.; Maes, A. Smolders, E., Role of soil constituents in fixation of soluble Zn, Cu, Ni and Cd added to soils. *Eur. J. Soil Sci.* **2007**, *58* (6), 1514−1524.

(16) Hoffmann, U.; Stipp, S. L. S. The behavior of Ni^{2+} on calcite surfaces. *Geochim. Cosmochim. Acta* **2001**, *65* (22), 4131−4139.

(17) Lee, S.; Lee, K.; Park, J. Simultaneous removal of Cd and Cr(VI) using Fe-loaded zeolite. *J. Environ. Eng. Div. (Am. Soc. Civ. Eng.)* **2006**, *132* (4), 445−450.

(18) Martinez, R. E.; Ferris, F. G. Review of the surface chemical heterogeneity of bacteriogenic iron oxides: Proton and cadmium sorption. *Am. J. Sci.* **2005**, *305* (6−8), 854−871.

(19) Randall, S. R.; Sherman, D. M.; Ragnarsdottir, K. V.; Collins, C. R. The mechanism of cadmium surface complexation on iron oxyhydroxide minerals. *Geochim. Cosmochim. Acta* **1999**, *63* (19−20), 2971−2987.

(20) Venema, P.; Hiemstra, T.; vanRiemsdijk, W. H. Multisite adsorption of cadmium on goethite. *J. Colloid Interface Sci.* **1996**, *183* (2), 515−527.

(21) Francis, A. J.; Dodge, C. J. Anaerobic microbial remobilization of toxic metals coprecipitated with iron-oxide. *Environ. Sci. Technol.* **1990**, *24* (3), 373−378.

(22) Tamaura, Y. Ferrite formation from the intermediate, green rust II, in the transformation reaction of gamma-FeO(OH) in aqueous suspension. *Inorg. Chem.* **1985**, *24* (25), 4363−4366.

(23) Verwey, E. J. W.; Heilmann, E. L. Physical properties and cation arrangement of oxides with spinel structures I. cation arrangement in spinels. *J. Chem. Phys.* **1947**, *15* (4), 174−180.

(24) Borch, T.; Kretzschmar, R.; Kappler, A.; Van Cappellen, P.; Ginder-Vogel, M.; Voegelin, A.; Campbell, K. Biogeochemical redox processes and their impact on contaminant dynamics. *Environ. Sci. Technol.* **2010**, *44* (1), 15−23.

(25) Weber, K. A.; Achenbach, L. A.; Coates, J. D. Microorganisms pumping iron: anaerobic microbial iron oxidation and reduction. *Nat. Rev. Microbiol.* **2006**, *4* (10), 752−764.

(26) Hohmann, C.; Winkler, E.; Morin, G.; Kappler, A. Anaerobic Fe(II)-oxidizing bacteria show As resistance and immobilize As during Fe(III) mineral precipitation. *Environ. Sci. Technol.* **2010**, *44* (1), 94−101.

(27) Konhauser, K. O.; Kappler, A.; Roden, E. E. Iron in microbial metabolisms. *Elements* **2011**, *7* (2), 89−93.

(28) Larese-Casanova, P.; Haderlein, S. B.; Kappler, A. Biomineralization of lepidocrocite and goethite by nitrate-reducing Fe(II)-oxidizing bacteria: Effect of pH, bicarbonate, phosphate, and humic acids. *Geochim. Cosmochim. Acta* **2010**, *74* (13), 3721−3734.

(29) Larese-Casanova, P.; Kappler, A.; Haderlein, S. B. Heterogeneous oxidation of Fe(II) on iron oxides in aqueous systems: Identification and controls of Fe(III) product formation. *Geochim. Cosmochim. Acta* **2012**, *91*, 171−186.

(30) Kappler, A.; Straub, K. L. Geomicrobiological cycling of iron. *Rev. Mineral. Geochem.* **2005**, *59*, 85−108.

(31) Zachara, J. M.; Fredrickson, J. K.; Smith, S. C.; Gassman, P. L. Solubilization of Fe(III) oxide-bound trace metals by a dissimilatory Fe(III) reducing bacterium. *Geochim. Cosmochim. Acta* **2001**, *65* (1), 75−93.

(32) Lloyd, J. R. Microbial reduction of metals and radionuclides. *FEMS Microbiol. Rev.* **2003**, *27* (2−3), 411−425.

(33) Fredrickson, J. K.; Zachara, J. M.; Kennedy, D. W.; Dong, H. L.; Onstott, T. C.; Hinman, N. W.; Li, S. M. Biogenic iron mineralization accompanying the dissimilatory reduction of hydrous ferric oxide by a groundwater bacterium. *Geochim. Cosmochim. Acta* **1998**, *62* (19−20), 3239−3257.

(34) Zachara, J. M.; Kukkadapu, R. K.; Fredrickson, J. K.; Gorby, Y. A.; Smith, S. C. Biomineralization of poorly crystalline Fe(III) oxides by dissimilatory metal reducing bacteria (DMRB). *Geomicrobiol. J.* **2002**, *19* (2), 179−207.

(35) Amstaetter, K.; Borch, T.; Kappler, A. Influence of humic acid imposed changes of ferrihydrite aggregation on microbial Fe(III) reduction. *Geochim. Cosmochim. Acta* **2012**, *85*, 326−341.

(36) Islam, F. S.; Gault, A. G.; Boothman, C.; Polya, D. A.; Charnock, J. M.; Chatterjee, D.; Lloyd, J. R. Role of metal-reducing bacteria in arsenic release from Bengal delta sediments. *Nature* **2004**, *430* (6995), 68−71.

(37) Fendorf, S.; Wielinga, B. W.; Hansel, C. M. Chromium transformations in natural environments: The role of biological and abiological. processes in chromium(VI) reduction. *Int. Geol. Rev.* **2000**, *42* (8), 691−701.

(38) Holmes, D. E.; Finneran, K. T.; O'Neil, R. A.; Lovley, D. R. Enrichment of members of the family *Geobacteraceae* associated with stimulation of dissimilatory metal reduction in uranium-contaminated aquifer sediments. *Appl. Environ. Microbiol.* **2002**, *68* (5), 2300−2306.

(39) Wang, X. J.; Chen, X. P.; Kappler, A.; Sun, G. X.; Zhu, Y. G. Arsenic binding to iron(II) minerals produced by an iron(III)-reducing *Aeromonas* strain isolated from paddy soil. *Environ. Toxicol. Chem.* **2009**, *28* (11), 2255−2262.

(40) Fendorf, S.; Michael, H. A.; van Geen, A. Spatial and temporal variations of groundwater arsenic in South and Southeast Asia. *Science* **2010**, *328* (5982), 1123−1127.

(41) Smedley, P. L.; Kinniburgh, D. G. A review of the source, behaviour and distribution of arsenic in natural waters. *Appl. Geochem.* **2002**, *17* (5), 517−568.

(42) Charlatchka, R.; Cambier, P. Influence of reducing conditions on solubility of trace metals in contaminated soils. *Water, Air, Soil Pollut.* **2000**, *118*, 143−167.
(43) Guo, T. Z.; DeLaune, R. D.; Patrick, W. H. The influence of sediment redox chemistry on chemically active forms of arsenic, cadmium, chromium, and zinc in estuarine sediment. *Environ. Int.* **1997**, *23* (3), 305−316.
(44) Lovley, D. R. Dissimilatory Fe(III) and Mn(IV) reduction. *Microbiol. Rev.* **1991**, *55* (2), 259−287.
(45) Burkhardt, E. M.; Bischoff, S.; Akob, D. M.; Buchel, G.; Küsel, K. Heavy metal tolerance of Fe(III)-reducing microbial communities in contaminated creek bank soils. *Appl. Environ. Microbiol.* **2011**, *77* (9), 3132−3136.
(46) Porsch, K.; Kappler, A. FeII oxidation by molecular O_2 during HCl extraction. *Environ. Chem.* **2011**, *8* (2), 190−197.
(47) Sabienë, N.; Brazauskienë, D. M.; Rimmer, D. Determination of heavy metal mobile forms by different extraction methods. *Ekologija* **2004**, *1*, 36−41.
(48) Harter, J.; Krause, H.-M.; Schuettler, S.; Ruser, R.; Fromme, M.; Scholten, T.; Kappler, A.; Behrens, S. Linking N2O emissions from biochar-amended soil to the structure and function of the N-cycling microbial community. *ISME J.* **2013**, DOI: 10.1038/ismej.2013.160.
(49) Stookey, L. L. Ferrozine-a new spectrophotometric reagent for iron. *Anal. Chem.* **1970**, *42* (7), 779−781.
(50) Abràmoff, M. D.; Magalhães, P. J.; Ram, S. J. Image processing with ImageJ. *Biophotonics Int.* **2004**, *11* (7), 36−42.
(51) Poulton, S. W.; Canfield, D. E. Development of a sequential extraction procedure for iron: implications for iron partitioning in continentally derived particulates. *Chem. Geol.* **2005**, *214* (3−4), 209−221.
(52) Moeslund, L.; Thamdrup, B.; Jorgensen, B. B. Sulfur and iron cycling in a coastal sediment - radiotracer studies and seasonal dynamics. *Biogeochemistry* **1994**, *27* (2), 129−152.
(53) Madigan, M. T.; Martinko, J. M. *Brock - Biology of microorganisms*, 11th ed.; Prentice-Hall, Inc.: Englewood Cliffs, NJ, 2006; p xvii, 909.
(54) Wetzel, R. G. Death, detritus, and energy-flow in aquatic ecosystems. *Freshwater Biol.* **1995**, *33* (1), 83−89.
(55) Lovley, D. R. Dissimilatory metal reduction. *Annu. Rev. Microbiol.* **1993**, *47*, 263−290.
(56) Roden, E. E.; Zachara, J. M. Microbial reduction of crystalline iron(III) oxides: Influence of oxide surface area and potential for cell growth. *Environ. Sci. Technol.* **1996**, *30* (5), 1618−1628.
(57) Schulz, K. G.; Riebesell, U.; Rost, B.; Thoms, S.; Zeebe, R. E. Determination of the rate constants for the carbon dioxide to bicarbonate inter-conversion in pH-buffered seawater systems. *Mar. Chem.* **2006**, *100* (1−2), 53−65.
(58) Kerner, M.; Wallmann, K. Remobilization events involving Cd and Zn from intertidal flat sediments in the Elbe estuary during the tidal cycle. *Estuarine, Coastal Shelf Sci.* **1992**, *35* (4), 371−393.
(59) McBride, M. B. Chemisorption of Cd^{2+} on calcite surfaces. *Soil Sci. Soc. Am. J.* **1980**, *44* (1), 26−28.
(60) Lindsay, W. L. *Chemical equilibria in soils*; John Wiley and Sons Ltd.: Chichester, Sussex, U. K., 1979.
(61) Wallmann, K. Solubility of cadmium and cobalt in a post-oxic or sub-oxic sediment suspension. *Hydrobiologia* **1992**, *235*, 611−622.
(62) Zhang, C. H.; Ge, Y.; Yao, H.; Chen, X.; Hu, M. K. Iron oxidation-reduction and its impacts on cadmium bioavailability in paddy soils: a review. *Front. Env. Sci. Eng.* **2012**, *6* (4), 509−517.
(63) Kasgoz, H.; Durmus, A.; Kasgoz, A. Enhanced swelling and adsorption properties of AAm-AMPSNa/clay hydrogel nanocomposites for heavy metal ion removal. *Polym. Adv. Technol.* **2008**, *19* (3), 213−220.
(64) Piepenbrock, A.; Dippon, U.; Porsch, K.; Appel, E.; Kappler, A. Dependence of microbial magnetite formation on humic substance and ferrihydrite concentrations. *Geochim. Cosmochim. Acta* **2011**, *75* (22), 6844−6858.
(65) Music, S.; Ristic, M. Adsorption of trace-elements or radionuclides on hydrous iron oxides. *J. Radioanal. Nucl. Chem.* **1988**, *120* (2), 289−304.
(66) Hennebel, T.; De Gusseme, B.; Boon, N.; Verstraete, W. Biogenic metals in advanced water treatment. *Trends Biotechnol.* **2009**, *27* (2), 90−98.
(67) Cutting, R. S.; Coker, V. S.; Telling, N. D.; Kimber, R. L.; Pearce, C. I.; Ellis, B. L.; Lawson, R. S.; Van der Laan, G.; Pattrick, R. A. D.; Vaughan, D. J.; Arenholz, E.; Lloyd, J. R. Optimizing Cr(VI) and Tc(VII) remediation through nanoscale biomineral engineering. *Environ. Sci. Technol.* **2010**, *44* (7), 2577−2584.
(68) Kanel, S. R.; Nepal, D.; Manning, B.; Choi, H. Transport of surface-modified iron nanoparticle in porous media and application to arsenic(III) remediation. *J. Nanopart. Res.* **2007**, *9* (5), 725−735.